Noise Effects on Quantum Encoded Image

Yayu Mo
ECE 7383 Introduction to Quantum Informatics
Southern Methodist University
Dallas, USA
yayum@mail.smu.edu

***Abstract*—The developments of quantum information dramatically impact the image processing field, however, challenges also occur. Especially in quantum image representation, the quantum noises interfere with the circuits that store images. In this paper, we explore the potential effects of quantum noise models on varied encodings, combining both quantum evaluation methodology and classical image evaluation method to find the pattern of noise behaviors affecting encodings. Furthermore, we also encode images on physical quantum machines to try to identify the noise channel that occurs compared with simulator patterns.**

***Index Terms*—quantum noise model, quantum image representation**

I. Introduction

In quantum computing, encoding classical images into quantum states has become a significant research perspective to exploit the advantages of quantum parallelism and entanglement. However, noise inherent in quantum systems, such as decoherence, operator errors and interactions with environments, poses significant challenges to maintaining the fidelity of quantum-encoded images.

Several works have been published to demonstrate the noise effects on varied algorithms. In 1997, Barenco et al.[1] related external environment noise with error correction algorithms, which further revealed the ultimate purpose of simulating noise in the encoded state is to construct an appropriate correction. They also introduce dephasing and arbitrary noise to support their error correction process. In 2010, the noise effects research had a dramatic flourish since Nielsen and Chuang[2] collected and analyzed general quantum noise channels in their famous 'Quantum Computation and Quantum Information' book. They modeled the noise as quantum operations in a quantum system interfered with the environment. Also in 2010, Quek et al.[3] explored the relationship between phasing noise sets (which refers to the combination of other noise channels and phase noise) and entanglement sudden death (ESD) in a Bell State.

Furthermore, noise effects were considered in the novel variational quantum approaches with varied data encodings. LaRose et al.[4] studied the behaviors of several data encodings, including angle, dense angle, amplitude, etc., for binary quantum classification and explored their properties both with and without noise. They also analyze the effects based on varied noise channels, including flips, depolarizing, amplitude damping, etc., to demonstrate the pattern when applying them to classifiers. In 2022, Wang et al.[5] explore the noise effects on the parameterized quantum circuit and inject noises at a gate-based level to observe the degradation and accuracy.

However, few of the works have related quantum noises with encoded images in quantum machines. This study explores the impact of various types of quantum noise models, including depolarizing model, amplitude damping, and phase damping, on quantum image encoding methods in both general and popular image representations. By analyzing the distinction in image quality and fidelity under different noise models, this research aims to provide insights into noise-resilient quantum encoding techniques, fostering advancements in quantum image processing and quantum error correction methods.

The article is organized in the following sections. In Sec. II, we briefly introduce the required backgrounds about concepts in quantum encodings and noise models. In Sec. III, we propose our approach to solve the problem and describe experimental arrangements, and then we introduce the dataset we apply in our experiments. In Sec. IV, several charts and tables are placed to show the result of our experiment. In Sec. V, we summarize the results and give a discussion for our future works.

II. Background

In this section, brief information about general quantum encodings, popular image representations, and quantum noise channels are introduced to help understand the concepts of our works.

A. Quantum Encoding

Encodings were often used in quantum memory to store data in a quantum machine and also applied as mapping to specific forms for algorithms and calculations.

In our work, we categorize the encodings into two types: classical encodings, which are basically proposed to store general data, and image representation encodings, specifically for storing images.

For classical encodings, as listed below:

- **Basis encoding**. The basis encoding was most widely used in classical quantum algorithms and calculations. It directly maps the binary bit string $x = b_{n-1}b_{n-2}...b_0$ to quantum state $|x\rangle = |b_{n-1}b_{n-2}...b_0\rangle$, which is quite simple to construct the circuit since only Pauli-X gate is needed to obtain the encoding.
- **Angle encoding**. Angle encoding has two types: general and dense encoding. The general angle encoding is also

known as the Qubit Lattice [6] in quantum image representations, which basically encodes normalized pixel values $\theta = \frac{x_i \pi}{180} \in [0, 2\pi)$ into amplitude performed by R_y gate, shown as

$$|\psi\rangle = \begin{bmatrix}\cos(\theta_0)\\ \sin(\theta_0)\end{bmatrix} \otimes \begin{bmatrix}\cos(\theta_1)\\ \sin(\theta_1)\end{bmatrix} \otimes \ldots \otimes \begin{bmatrix}\cos(\theta_{n-1})\\ \sin(\theta_{n-1})\end{bmatrix} \quad (1)$$

The same as basis encoding, the required qubit numbers of general encoding equal to the data size. To tackle that problem, we have dense angle encoding, which encodes odd data as a phase ϕ in $|1\rangle$, shown as

$$|\psi_j\rangle = \begin{bmatrix}\cos(\theta_{2j})\\ e^{i\phi_2 j+1}\sin(\theta_{2j})\end{bmatrix} \quad (2)$$

- **Amplitude encoding**. Also proposed as quantum probability image encoding (QPIE) [7], the amplitude encoding puts data into a superposition with the intensity of data mapping as amplitude coefficients and index as j^{th} state. Compared with basis encoding, it could directly map data as statevectors without converting to binary form, and with the advantage of superposition, it has the capability of storing 2^n data points using only n qubits. However, the amplitude encoding is complicated to construct with a depth of $\mathcal{O}(2^n)$.
- **QUAM encoding**. Quantum associative memory is also based on superposition, it puts the ordered data sequence into even probabilities of superposition. With the advantage of superposition, the qubit number required highly depends on the length of the binary-converted data elements. However, the core limitations of this encoding are also obvious; it's hard to determine the coordinates of the original data after encoding, especially when encountering repeatable data; for example, if several coordinates have the same intensity value in images, it would be hard to retrieve images from the quantum state.
- **QRAM encoding**. Compared with QUAM, quantum random access memory has further encoded addresses that are aligned with data. Because of the benefits of using addresses-data pairs, it is able to encode $2^n \times m$ data dimensions. Based on the advantages, we explore a novel efficient-QRAM circuit proposed by Zidan et al.[8] to show the distinct result from NEQR image representation, which is also another form of QRAM or QROM that we are going to discuss later.
- **Angle QRAM encoding**. Angle QRAM encoding changes the encodings of data part from basis encoding to dense angle encoding. With the benefit of 2 data points in a single qubit by dense angle encoding, we are able to further decrease half of the number of the qubits in the data part.

Several popular image representation approaches are introduced as follows:

- **FRQI**. In 2011, Li et al.[4] proposed a flexible representation of quantum images (FRQI) with a similar form as angle QRAM but only put the data in the general angle encodings, which means it maps image intensity to amplitude and a tensor product with $|i\rangle$ in encoding represents coordinate information.
- **MCRQI**. To encode images in color spaces, Sun et al.[9] proposed a multi-channel representation of quantum images (MCRQI). The author encodes four channels of red, green, blue and transparency $(\alpha) \in [0, 255]$ into angles $\Theta = \{\theta_{R_i}, \theta_{G_i}, \theta_{B_i}, \theta_{\alpha_i}\} \in [0, \frac{\pi}{2}]$. The color space state of i^{th} pixel could be shown as

$$\left|c^i_{RGB\alpha}\right\rangle = \frac{1}{2}\Big(\sum_{\substack{\theta\in\Theta,\\ x\in\{0,1\}^2}} (\cos\theta\,|0\rangle + \sin\theta\,|1\rangle) \otimes |x\rangle\Big) \quad (3)$$

Since the color channels have to be measured separately and with the encoding's similarity with FRQI, the encoding has the most complicated circuit depth of $4 \times 2^{4(n+1)} - 6 \times 2^{2(n+1)} + 2(n+1)$.
- **NEQR**. Novel enhanced quantum representation of digital images (NEQR) [10] has a similar quantum state format as QRAM. With the benefits of QRAM, it is able to encode images with less quantized noise, which basically reverts the images from distribution keys other than distribution values, which are the main image reversion bases for other image encodings.
- **QSMC-QSNC**. Li et al.[11] proposed quantum states for M colors (QSMC) and for N coordinates (QSNC). Both the intensities and coordinates are stored in the same form by R_y gate as $\{\phi, \theta\}$ and correlated after being encoded separately. The core potential of this method, which deals with image compression problems and image segmentation methods based on Grover's search algorithm[12], has been verified by the author.
- **BRQI**. Inspired by NEQR, a bitplane representation of quantum images (BRQI) was suggested by Li et al.[13]. It splits the image into n bitplanes, which j^{th} bitplane is defined in Table II. The encoding means it maps every k^{th} bit position accordingly into the $n \times n$ bit plane. To better understand it, the bitplane BP could also be shown as

$$I = \{b_{0,0}...b_{0,7}, ..., b_{(n-1)^2,0}...b_{(n-1)^2,7}\} \rightarrow$$
$$BP_i = \begin{bmatrix} b_{0,i} & b_{1,i} & \cdots & b_{n-1,i} \\ b_{n,i} & b_{n+1,i} & \cdots & b_{2(n-1),i} \\ \vdots & \vdots & \ddots & \vdots \\ b_{(n-2)(n-1),i} & b_{(n-2)(n-1)+1,i} & \cdots & b_{(n-1)^2,i} \end{bmatrix} \quad (4)$$

- **OQIM**. Xu et al.[14] proposed an order-encoded quantum image model (OQIM) to store sorted intensities and coordinates of images in θ and ϕ, respectively, in a single qubit, shown as

$$(\cos\theta_i\,|0\rangle + \sin\theta_i\,|1\rangle) \otimes |0\rangle + (\cos\phi_i\,|0\rangle + \sin\phi_i\,|1\rangle) \otimes |1\rangle \quad (5)$$

From the equation and quantum state in Table II, the encoding combines the benefits of both angle encoding and angle QRAM to be more flexible in the image enhancement method.

For more detail, we listed the quantum state and required qubits of general encodings and image representations in Table I and Table II.

B. Quantum Noise channel

In a quantum system, noises that a quantum system interacts with environments could be modeled as quantum operations. Taking the environment into consideration, quantum operations can further be represented as operator-sum representation, written as

$$\begin{aligned}\varepsilon(\rho) &= \sum_k \langle e_k| U[\rho \otimes |e_0\rangle \langle e_0|]U^\dagger |e_k\rangle \\ &= \sum_k E_k \rho E_k^\dagger\end{aligned} \tag{6}$$

where $|e_k\rangle$ is an orthonormal basis for the state space of the environment, $|e_0\rangle \langle e_0|$ represents the initial mixed state of the environment, and $E_k = \langle e_k| U |e_0\rangle$ is an operator on the state space after inherent with environment, also known as the operation elements for quantum operation ε. In this case, the environmental model could be modeled as the circuit in Fig. 1.

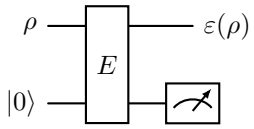

Fig. 1: Environmental model for a quantum operation

We list several well-known channels for quantum noise models as follows [2]:

- **Bit Flip and Phase Flip channels**. In this channel, we take bit flip as an example; the nature of bit flip is that the noise would occur with the probability of $1-p$, which has the behavior of flipping the state $|0\rangle$ to $|1\rangle$ (or $|1\rangle$ to $|0\rangle$. It has operation elements

$$E_0 = \sqrt{p} I = \sqrt{p} \begin{bmatrix} 1 & 0 \\ 0 & 1 \end{bmatrix} \tag{7}$$

$$E_1 = \sqrt{1-p} X = \sqrt{1-p} \begin{bmatrix} 0 & 1 \\ 1 & 0 \end{bmatrix} \tag{8}$$

  The phase flip and bit-phase flip also has the same operation elements but changes the Pauli-X to Pauli-Z for phase flip and Pauli-Y for bit-phase flip.
- **Depolarization channel**. The depolarization channel also has the behavior of the occurrence with the probability p that qubit is depolarized, but the difference is that it's replaced by the completely mixed state, $I/2$. The state of noised quantum system can be shown as

$$\varepsilon(\rho) = \frac{pI}{2} + (1-p)\rho \tag{9}$$

  and the circuit implementation is shown in Fig. 2.

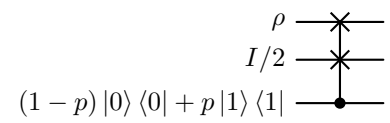

Fig. 2: Circuit for depolarization channel

- **Amplitude Damping channel**. The core influence of amplitude damping is the loss of energy, which is called energy dissipation in quantum dynamics. In a zero temperature, the quantum operation over the environment could be represented as

$$\varepsilon_{AD}(\rho) = E_0 \rho E_0^\dagger + E_1 \rho E_1^\dagger \tag{10}$$

  where $E_k = \langle k| U |0\rangle$ are

$$E_0 = \begin{bmatrix} 1 & 0 \\ 0 & \sqrt{1-\gamma} \end{bmatrix} \quad E_1 = \begin{bmatrix} 0 & \sqrt{\gamma} \\ 0 & 0 \end{bmatrix} \tag{11}$$

  where $\gamma = \sin^2\theta$. So that it could be modeled as Fig. 3. For finite temperature, which is a more generalized case,

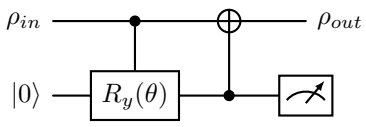

Fig. 3: Circuit for amplitude damping

  consider a single qubit pure state $\rho = (1-p)I + (2p-1)|0\rangle\langle 0|$, in this case,

$$\varepsilon_{GAD}(U\rho U^\dagger) = (1-p)I + (2p-1)\varepsilon_{AD}(U\rho U^\dagger) \tag{12}$$

- **Phase Damping channel**. The phase damping channel describes the loss of quantum information without loss of energy. And the operation elements E_k can be shown as

$$E_0 = \begin{bmatrix} 1 & 0 \\ 0 & \sqrt{1-\lambda} \end{bmatrix} \quad E_1 = \begin{bmatrix} 0 & 0 \\ 0 & \sqrt{\lambda} \end{bmatrix} \tag{13}$$

  where $\lambda = 1 - \cos^2(\chi \Delta t)$ represents the loss of information. The phase damping circuit is shown as Fig. 4.

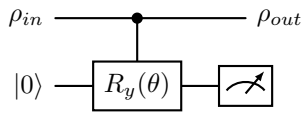

Fig. 4: Circuit for phase damping

III. Approach

A. Circuit Evaluation

The circuit evaluation is mainly divided into two parts: circuit depth and qubit numbers.

- **Circuit depth** describes the total length of parallel operations evolving from the initial state to the end state. In general cases, a larger depth means the circuit is more

TABLE I: General Encodings

Encodings	Quantum State	Required Qubits
Basis Encoding	$x \in \mathbb{Z}_2^n \rightarrow \lvert b_{n-1}b_{n-2}...b_0\rangle$	$l = n$
Angle Encoding	$x \in [0, 2\pi) \rightarrow \otimes_{j=0}^{N-1} \cos(x_j)\lvert 0\rangle + \sin(x_j)\lvert 1\rangle$	$l = n$
	$x \in [0, 2\pi) \rightarrow \otimes_{j=0}^{(N-2)/2} \cos(x_{2j})\lvert 0\rangle + e^{ix_{2j+1}} \sin(x_{2j})\lvert 1\rangle$	$l = n/2$
Amplitude Encoding	$x \rightarrow \sum_{j=0}^{n-1} c_j \lvert j\rangle, c_i = \frac{x_j}{\sqrt{\sum x_j^2}}$	$l = \log_2(n)$
QUAM	$x_j \in \mathbb{Z}_2^m \rightarrow \sum_{j=0}^{n-1} \frac{1}{\sqrt{n}} \lvert x_j\rangle$	$l = m$
QRAM	$a_j \in \mathbb{Z}_2^n, x_j \in \mathbb{Z}_2^m \rightarrow \sum_{j=0}^{n-1} \frac{1}{\sqrt{n}} \lvert a_j\rangle \lvert x_j\rangle$	$l = 2(\log_2(n) + m) + 2$
Angle QRAM	$a_j \in \mathbb{Z}_2^n, x_j \in [0, 2\pi) \rightarrow \sum_{j=0}^{(n-2)/2} (\cos(x_{2j+1})\lvert 0\rangle + e^{ix_{2j}} \sin(x_{2j+1})\lvert 1\rangle) \otimes \lvert a_j\rangle$	$l = 2(log2(n) + m/2) + 2$

TABLE II: Image Representations

Encodings	Quantum State	Required Qubits
FRQI [4]	$I(x_i) \rightarrow \frac{1}{2^n} \sum_{i=0}^{2^2n-1} (\cos x_i \lvert 0\rangle + \sin x_i \lvert 1\rangle) \otimes \lvert i\rangle$	$l = \log_2(n^2) + 1$
MCRQI [9]	$I(\theta) = \frac{1}{2^n} \sum_{i=0}^{2^2n-1} \left\lvert c^i_{RGB_x}\right\rangle \otimes \lvert i\rangle$	$l = 2\log_2(n) + 8$
NEQR [10]	$I(x, y) = \frac{1}{2^n} \sum_{y=0}^{2^n-1} \sum_{x=0}^{2^n-1} \otimes_{i=0}^{q-1} \lvert c^i_{x,y}\rangle \lvert i_{x,y}\rangle$	$l = 2\log_2(n) + 8$
QSMC-QSNC [11]	$\lvert v_i\rangle = R_y(2\phi_i), \lvert u_i\rangle = R_y(2\theta_i) \rightarrow \lvert \psi_i\rangle = \lvert v_i\rangle \otimes \lvert u_i\rangle$	$l = \log_2(n^2) + 2$
BRQI [13]	$\left\lvert \Psi^j\right\rangle = \frac{1}{\sqrt{2^n}} \sum_{x=0}^{2^{n-k}-1} \sum_{y=0}^{2^k-1} \lvert g(x, y)\rangle \lvert x\rangle \lvert y\rangle$	$l = 2\log_2(n) + 4$
OQIM [14]	$I(\theta, \phi) \rightarrow \frac{1}{2^{n+1/2}} \sum_{i=0}^{2^2n-1} (\cos\theta_i \lvert 00\rangle + \sin\theta_i \lvert 10\rangle + \cos\phi_i \lvert 01\rangle + \sin\phi_i \lvert 11\rangle) \otimes \lvert i\rangle$	$l = \log_2(n^2) + 2$

Fig. 5: Orignial image for testing.

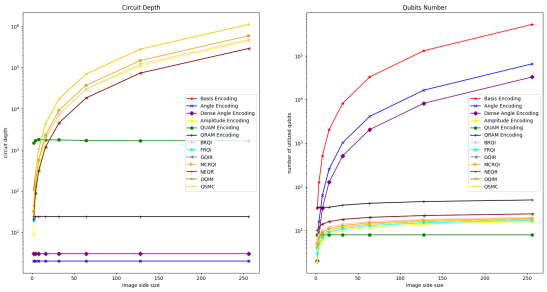

Fig. 6: Circuit evaluation curve

complicated and has a higher time complexity for both construction and propagation.

- **Qubit numbers** describes the width of a circuit. Usually, physical quantum computers have limited numbers of qubits, but through simulation, we could calculate the theoretical high level of required qubits for different sizes of images

Circuit depth and qubits number could be varied with different image sizes and intensity distributions. In our work, we apply a sequence of image side sizes from 2^1 to 2^8 of a rescaled 256x256x3 Psyduck image (shown as Fig. 5) due to the reason that it has simple curves and centered intensity distributions which could perform well in most of the encodings.

Some of the encodings have pretty diverse depth or qubits numbers. To distinguish the difference between high-level and low-level, we apply an automated logarithm in the y-axis in the evaluation results, shown as Fig. 6

B. Noised Circuit Test

Noise could be applied to several perspectives like gates, measurements, reset even readout processes. In our work, we focus on the gates and measurements part. According to the quantum state, we could assume that some quantum channels could happen much more frequently than others. For example, amplitude encoding would have a much higher probability of amplitude damping problems in the measurement stage, or basis encoding is more likely to occur bit-flip in a gate base.

According to the circumstances above, the test procedure is shown in Table. III

C. Noise Effect Evaluation

In this section, we apply mean squared error (MSE) and structural similarity index measure (SSIM) to compare the noisy images with quantized images for the noise effect

TABLE III: Test Settings

Encodings	Noise Models	Base
Basis	bit-flip	gates
Angle	amplitude damping	gates&measurement
Dense Angle	amplitude damping	gates&measurement
	phase flip&damping	gates
Amplitude	amplitude damping	gates&measurement
QUAM	depolarizing	gates
Efficient QRAM	depolarizing	gates
Angle QRAM	depolarizing	gates
	amplitude damping	gates&measurement
	phase flip&damping	gates
FRQI	depolarizing	gates
	amplitude damping	gates&measurement
MCRQI	depolarizing	gates
	amplitude damping	gates&measurement
NEQR	depolarizing	gates
QSMC-QSNC	amplitude damping	gates&measurement
BRQI	bit-flip	gates
	depolarizing	gates
OQIM	depolarizing	gates
	amplitude damping	gates&measurement

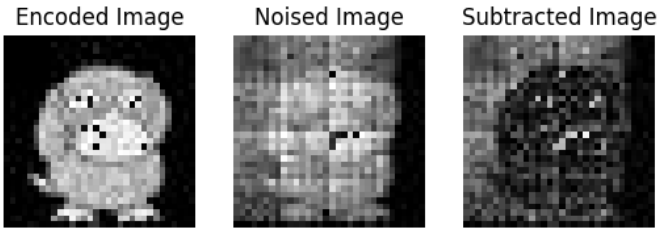

Fig. 7: Quantized images in amplitude encoding in amplitude damping noise with a parameter of 0.15 injected in measurement part.

evaluation part, denoted as

$$\begin{aligned} MSE(x,y) &= \frac{1}{mn}\sum_{i=0}^{m-1}\sum_{j=0}^{n-1}[x_{i,j}-y_{i,j}]^2 \\ SSIM(x,y) &= \frac{(2\mu_x\mu_y+c_1)(2\sigma_{xy}+c_2)}{(\mu_x^2+\mu_y^2+c_1)(\sigma_x^2+\sigma_y^2+c_2)} \end{aligned} \tag{14}$$

where in SSIM, μ represents the pixel sample mean, and σ represents the variance for a single sample window or covariance for both x and y windows. Specifically for c_1, c_2, which are two variables to stabilize the division with weak denominator. Since they highly depend on the dynamic range L of the pixel values, c_1 and c_2 could be denoted as

$$c_1 = (k_1 L)^2, \quad c_2 = (k_2 L)^2 \tag{15}$$

where $k_1 = 0.01$ and $k_2 = 0.03$ by default are two constant coefficients.

In addition, we also calculate the per-pixel absolute subtraction between noised images and quantized images to observe the pattern after injected noise, shown as Fig. 7.

D. Experiment settings on dataset

For non-rotation-based encodings, which means the circuit is not parameterized in rotation gates, the circuit would vary in depth and even qubit numbers when different images are applied to them. Evaluating the overall effects on a set of images is significant in seeking the general pattern for noisy images, so we plan to apply different noise channels to the dataset encoded in amplitude encoding, which has even time complexity for both constructing and propagating.

E. Test on real machine

To compare the simulator with the real environment and try to identify the patterns for noise models, we plan to test on the QisKit H1 series and the Tket Ion trap machine, and since Tket has the extension for the Qiskit package that is able to migrate circuits from one to another, we focus most on Qiskit to construct the circuit.

F. Datasets

Except for the Psyduck image for testing, we also apply the Linnaeus 5 dataset [15] for evaluating the overall effects of varied noise on encodings. The dataset includes 1600 images with the shape of 256x256x3, and it was originally used for classification tasks. The reason for applying it as our evaluation dataset is that the images follow the regulation of $2^n \times 2^n$, which perfectly fits the requirements for most of the encodings. In addition, considering the qubit numbers of real machines that have been achieved, such as IBM Brisbane with 127 qubits, QuEra Aquila with 256 qubits, etc., it's reasonable to exploit the images with a shape that fits the quantum machines.

IV. Result

In processing...

V. Summary

In this paper, we explore the effects of varied quantum noise channels on several quantum encoding and image representation methods. We also evaluate the tendency of distinction when increasing parameters and obtain the patterns in subtraction. Furthermore, we also evaluate the overall performance in the dataset to seek the general pattern for the effects since circuits are highly correlated with images that are going to be encoded. For the last part, we test our encodings on real machines to compare and try to identify the patterns. Our future work will be focusing on noise-resilient image representations, which means denoising or error correction according to the pattern of this work.

References

[1] Adriano Barenco, Todd A Brun, Rüdiger Schack, and Timothy P Spiller. Effects of noise on quantum error correction algorithms. *Physical Review A*, 56(2):1177, 1997.

[2] Michael A Nielsen and Isaac L Chuang. *Quantum computation and quantum information*. Cambridge university press, 2010.

[3] Sylvanus Quek, Ziang Li, and Ye Yeo. Effects of quantum noises and noisy quantum operations on entanglement and special dense coding. *Physical*

Review A—Atomic, Molecular, and Optical Physics, 81(2):024302, 2010.

[4] Phuc Q Le, Fangyan Dong, and Kaoru Hirota. A flexible representation of quantum images for polynomial preparation, image compression, and processing operations. *Quantum Information Processing*, 10:63–84, 2011.

[5] Hanrui Wang, Jiaqi Gu, Yongshan Ding, Zirui Li, Frederic T Chong, David Z Pan, and Song Han. Quantumnat: quantum noise-aware training with noise injection, quantization and normalization. In *Proceedings of the 59th ACM/IEEE design automation conference*, pages 1–6, 2022.

[6] Salvador E Venegas-Andraca and Sougato Bose. Storing, processing, and retrieving an image using quantum mechanics. In *Quantum information and computation*, volume 5105, pages 137–147. SPIE, 2003.

[7] Xi-Wei Yao, Hengyan Wang, Zeyang Liao, Ming-Cheng Chen, Jian Pan, Jun Li, Kechao Zhang, Xingcheng Lin, Zhehui Wang, Zhihuang Luo, et al. Quantum image processing and its application to edge detection: theory and experiment. *Physical Review X*, 7(3):031041, 2017.

[8] Mohammed Zidan, Abdel-Haleem Abdel-Aty, Ashraf Khalil, Mahmoud Abdel-Aty, and Hichem Eleuch. A novel efficient quantum random access memory. *Ieee Access*, 9:151775–151780, 2021.

[9] Bo Sun, Phuc Q Le, Abdullah M Iliyasu, Fei Yan, J Adrian Garcia, Fangyan Dong, and Kaoru Hirota. A multi-channel representation for images on quantum computers using the rgbα color space. In *2011 IEEE 7th International Symposium on Intelligent Signal Processing*, pages 1–6. IEEE, 2011.

[10] Yi Zhang, Kai Lu, Yinghui Gao, and Mo Wang. Neqr: a novel enhanced quantum representation of digital images. *Quantum information processing*, 12:2833–2860, 2013.

[11] Hai-Sheng Li, Zhu Qingxin, Song Lan, Chen-Yi Shen, Rigui Zhou, and Jia Mo. Image storage, retrieval, compression and segmentation in a quantum system. *Quantum information processing*, 12(6):2269–2290, 2013.

[12] Lov K Grover. A fast quantum mechanical algorithm for database search. In *Proceedings of the twenty-eighth annual ACM symposium on Theory of computing*, pages 212–219, 1996.

[13] Hai-Sheng Li, Xiao Chen, Haiying Xia, Yan Liang, and Zuoshan Zhou. A quantum image representation based on bitplanes. *IEEE access*, 6:62396–62404, 2018.

[14] Guanlei Xu, Xiaogang Xu, Xun Wang, and Xiaotong Wang. Order-encoded quantum image model and parallel histogram specification. *Quantum Information Processing*, 18:1–26, 2019.

[15] G Chaladze and L Kalatozishvili. Linnaeus 5 dataset for machine learning. *chaladze. com*, 2017.